Structural Engineering and Mechanics, *Vol. 55, No. 2 (2015) 435-459*
DOI: http://dx.doi.org/10.12989/sem.2015.55.2.435

Parametric resonance of composite skew plate under non-uniform in-plane loading

Rajesh Kumar[1], Abhinav Kumar[2] and Sarat Kumar Panda[*2]

[1]*Department of Civil Engineering, Indian Institute of Technology Kharagpur, India*
[2]*Department of Civil Engineering, Indian School of Mines Dhanbad, India*

(Received December 1, 2014, Revised June 22, 2015, Accepted June 23, 2015)

Abstract. Parametric resonance of shear deformable composite skew plates subjected to non-uniform (parabolic) and linearly varying periodic edge loading is studied for different boundary conditions. The skew plate structural model is based on higher order shear deformation theory (HSDT), which accurately predicts the numerical results for thick skew plate. The total energy functional is derived for the skew plates from total potential energy and kinetic energy of the plate. The strain energy which is the part of total potential energy contains membrane energy, bending energy, additional bending energy due to additional change in curvature and shear energy due to shear deformation, respectively. The total energy functional is solved using Rayleigh-Ritz method in conjunction with boundary characteristics orthonormal polynomials (BCOPs) functions. The orthonormal polynomials are generated for unit square domain using Gram-Schmidt orthogonalization process. Bolotin method is followed to obtain the boundaries of parametric resonance region with higher order approximation. These boundaries are traced by the periodic solution of Mathieu-Hill equations with period T and 2T. Effect of various parameters like skew angle, span-to-thickness ratio, aspect ratio, boundary conditions, static load factor on parametric resonance of skew plate have been investigated. The investigation also includes influence of different types of linearly varying loading and parabolically varying bi-axial loading.

Keywords: skew plate; BCOPs, parametric resonance; non-uniform in-plane loading; dynamic instability

1. Introduction

The composite plate is very well known in research community due to their beneficial properties such as high strength to weight ratio, high in-plane stiffness, damping, and their directional properties. Composite skew plates are used widely in many practical applications e.g., aircrafts, space vehicles, missiles, high-speed air craft and many complex structures. During their operational life, these structures are subjected to non-uniform in-plane static and dynamic loadings. For proper designing and evaluating the performances of structural systems, studies of parametric resonance of skew plates of different boundary conditions due to non-uniform and linearly varying in-plane loadings are important.

∗Corresponding author, Assistant Professor, E-mail: sarat.iitm@gmail.com, panda.sk.civ@ismdhanbad.ac.in

http://www.techno-press.org/?journal=sem&subpage=8 ISSN: 1225-4568 (Print), 1598-6217 (Online)

A number of research articles have been published on the parametric resonance characteristic of different rectangular plates using Bolotin's method (Bolotin 1964). Srinivasan and Chellapadi (1986) investigated the dynamic instability of rectangular laminated composite plate subjected to uniform in-plane periodic loading using finite strip method (FSM). Bert and Birman (1987) studied the effect of shear deformation on the dynamic instability of simply supported anti-symmetric angle-ply rectangular plates subjected to uniform in-plane periodic loading using Galerkin's method. Takahashi and Konishi (1988) presented the dynamic instability of rectangular plate subjected to linearly varying in-plane periodic load. Moorthy *et al*. (1990) investigated the parametric instability of laminated composite plate under uniform in-plane load using finite element method. Chen and Yang (1990) presented the dynamic instability of laminated composite plates subjected to combine in-plane periodic compressive stress and bending stress. Ganapathi *et al*. (1999) worked on the non-linear dynamic instability of laminated composite plate under uniform in-plane periodic load under the framework of finite element method. Radu and Chattopadhyay (2002) studied the dynamic instability of delaminated composite under uniform in-plane periodic loading using finite element method. Prakash and Ganapathi (2005) presented the dynamic instability characteristics of aero-thermo-mechanically stressed functionally graded plates using finite element procedure. Patel *et al*. (2006) investigated the dynamic instability characteristics of laminated composite stiffened shell panels subjected to in-plane harmonic edge loading within the frame work of finite element method. Udar and Datta (2007) investigated the problem of the occurrence of combination resonances in contrast to simple resonances in parametrically excited doubly curved panels subjected to non-uniform tensile in-plane harmonic edge loading. Ramachandra and Panda (2012) investigated dynamic instability of shear deformable composite plate subjected to non-uniform in-plane periodic loading. Here, the authors followed Galerkin's method to reduce the partial differential equations into Mathieu type equations and Bolotin's method was employed to trace the four zones of dynamic instability. Wang *et al*. (2013) studied the static and dynamic characteristics of composite plates subjected to an arbitrary periodic load in hygrothermal environments. The authors determined the regions of dynamic instability of the composite plate by solving the eigenvalue problems based on Bolotin's method. Chen *et al*. (2013) studied the dynamic instability of laminated composite plates under thermal and arbitrary in-plane periodic loads using first-order shear deformation plate theory. The authors used Galerkin's method in conjunction with Bolotin's method to determine dynamic instability regions of laminated plates in the thermal environment.

There are many research works carried out on buckling and vibration of skew plate. Durvasula (1971) investigated the buckling problems of simply supported skew plates using the Rayleigh-Ritz method, employing a double fourier sine series in oblique coordinates. Liew and Lam (1990) investigated the flexural vibration of skew plates by Rayleigh-Ritz method and followed Gram-Schmidt orthogonalization process to generate two-dimensional orthogonal plate functions. Wang *et al.* (1992) worked on buckling of skew plates and corner conditions for simply supported edges by using Rayleigh-Ritz method. Flexural vibration of skew plates using boundary characteristic orthogonal polynomials in two variables is investigated by Singh and Chakraverty (1994). Wang (1997) used B-spline function in conjunction with Rayleigh-Ritz method for buckling analysis of skew composite laminated plates using first order shear deformation theory. Babu and Kant (1999) studied on two shear deformable finite element models for buckling analysis of skew fiber-reinforced composite and sandwich panels. Buckling and transverse vibration of orthotropic non-homogeneous rectangular plates of variable thickness are presented by Kumar and Lal (2011). Here, the author analysed the plate using two dimensional boundary characteristic orthogonal

polynomials in Rayleigh-Ritz method.

Parametric resonance of composite skew plates has been investigated by many researchers. The parametric resonance of skew plate is considered first time by Merrit and Willems (1973) under uniform in-plane periodic loading. Liao and Cheng (1994) studied the influence of skew angle, stiffness scheme, lamination scheme on the dynamic instability of laminated composite plates and shells under uniform in-plane periodic load using 3-D degenerated curved shell element. Dey and Singha (2006) presented the parametric resonance regions of skew plates subjected to uniform periodic in-plane load using finite element approach. The authors investigated the skew plate with second order approximation i.e. first two terms of the fourier series of the assumed periodic solution has been considered. Wu and Shih (2006) obtained parametric resonance and non-linear response of laminated skew plates under periodic uniform in-plane loading. Galerkin's method with proper mode shapes was employed and the governing partial differential equations were reduced into Mathieu equations. Incremental harmonic balance method is used to solve the non-linear temporal equations of motion to obtain the region of parametric resonance. Lee (2010) studied the parametric resonance of laminated composite skew plate with central cut-out subjected to periodic uniform in-plane load using finite element method based on higher order shear deformation theory (HSDT). Noh and Lee (2014) analysed the parametric resonance of delaminated composite skew plate subjected to periodic uniform in-plane loading using finite element method based on HSDT. Authors investigated the skew plate with first order approximation and followed Bolotin's method to plot the instability zones.

In actual structures plates are a part of complex structural system and hence load coming on it is non-uniform. There is no work available in open literature on parametric resonance of skew plates under non-uniform in-plane edge loading. In the present investigation, parametric resonance of skew plates under parabolic and linearly varying edge loading is considered. Since the applied in-plane edge load is not uniform, the resultant plate in-plane stresses distribution (σ_ξ, σ_η and $\tau_{\xi\eta}$) within the composite skew plate are evaluated from plane elasticity problem by minimizing the membrane strain energy using Ritz method. The total potential energy functional of the skew plate is transformed from physical domain to computational domain using transformation equation. The orthonormal polynomials are generated by using Gram-Schmidt orthogonalization process. Boundary characteristics orthonormal polynomials (BCOPs) functions consist of the product of two dimensional linearly independent set of polynomial functions and a basis function. The basis function is formed from taking the product of the equations of the boundaries. To satisfying the essential boundary condition, each equation of the boundary is raised to the power of 0, 1 or 2 corresponding to free, simply supported, or clamped edges. Following Rayleigh-Ritz method with BCOPs functions are used to reduce the total energy functional to ordinary differential equations (Mathieu-Hill equations). The boundaries of parametric resonance are traced by periodic solution of Mathieu-Hill equations with period T and 2T. The results are presented for different skew angles, span-to-thickness ratio, aspect ratio, static load factor, boundary conditions and various types of loadings on parametric resonance. Influence of biaxial loading on the boundary of parametric resonance is also investigated.

2. Formulation

Laminated skew plate of length 'a', width 'b' and composed of n layers of equal thickness is considered with the co-ordinate axes ξ-η in the in-plane directions and the z-axis in the thickness

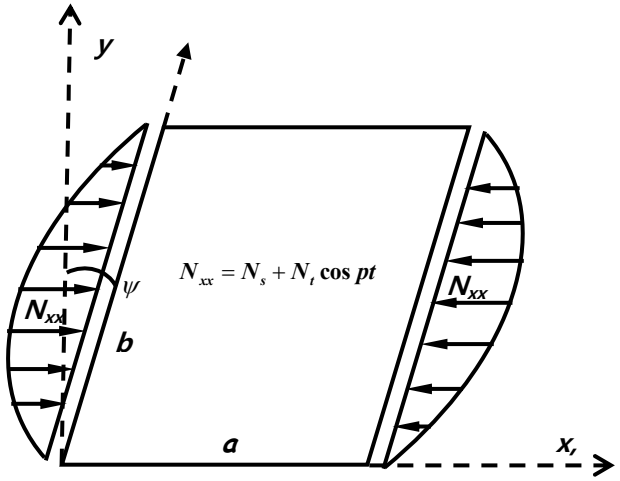

Fig. 1(a) Geometry and parabolic periodic in-plane loading of the plate

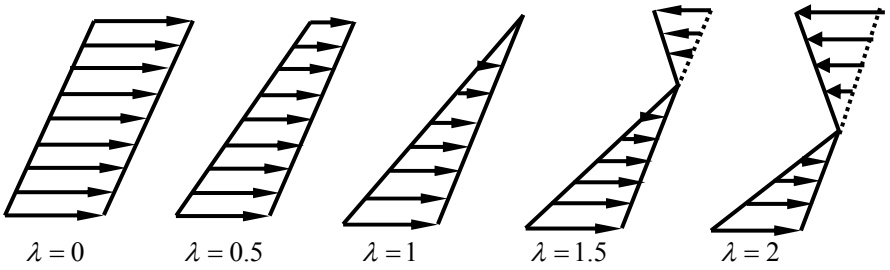

Fig. 1(b) Different type of linearly varying loading considered

direction of the plate. The skew plate is edge loaded with parabolic in-plane loading as shown in Fig. 1(a).

The different types of in-plane loading distributions studied in the present investigation other than parabolic in-plane loading are given in Fig. 1(b). The in-plane edge loading may be expressed as: $N_{xx} = N_0(1-\lambda(\frac{\eta}{b}))$. By taking various values of λ, we obtain different in-plane load distribution: uniform (λ=0), trapezoidal (λ=0.5), triangular (λ=1), partial tension (λ=1.5) and in-plane bending (λ=2). For λ=1.5 and λ=2.0, some portion of the plate edge (dotted line) is subjected to tension as shown in Fig. 1(b).

In the present investigation the higher-order shear deformation theory (HSDT) for laminated composite plates as proposed by Reddy and Liu (1985) is adopted. In this theory, the displacements of the middle surface are expanded as cubic functions of the thickness coordinate and the transverse displacement is assumed to be constant through the thickness. This displacement fields leads to the parabolic distribution of the transverse shear stress and zero transverse normal strain and hence no shear correction factors are used. The displacement fields may be written as

$$u = u^o + z\varphi_1 + z^3(4/3h^2)[-\varphi_1 - w^o_{,x}]$$

$$\begin{aligned} v &= v^o + z\varphi_2 + z^3(4/3h^2)[-\varphi_2 - w^o_{,y}] \\ w &= w^o \end{aligned} \tag{1}$$

The above displacement fields can be rearranged as Soldatos (1991)

$$\begin{aligned} u &= u^o - zw^o_{,x} + f(z)\phi_1{}^o \\ v &= v^o - zw^o_{,y} + f(z)\phi_2{}^o \\ w &= w^o \end{aligned} \tag{2}$$

$$\text{where } \phi_1^0 = \varphi_1 + w^0_{,x} \;;\; \phi_2^0 = \varphi_2 + w^0_{,y} \text{ and } f(z) = z[1-(4/3)(z/h)^2] \tag{3}$$

Here u, v and w are displacement components along x, y, z directions respectively at a distance z away from mid plane and u^0, v^0 and w^0 are displacement component of a generic point on the middle surface. φ_1 and φ_2 are rotations of the cross sections initially perpendicular to the x and y axes respectively. h is the thickness of the plate and $(\,)_{,x}$ represents the differentiation with respect to x. The linear strain-displacement relations at a distance 'z' away from the mid-plane of a plate can be written as

$$\begin{aligned} \varepsilon_x &= \varepsilon^o_x - zw^o_{,xx} + f(z)\phi^o_{1,x} \\ \varepsilon_y &= \varepsilon^o_y - zw^o_{,yy} + f(z)\phi^o_{2,y} \\ \gamma_{xy} &= \gamma^o_{xy} - 2zw^o_{,xy} + f(z)\phi^o_{1,y} + f(z)\phi^o_{2,x} \\ \gamma_{xz} &= u_{,z} + w_{,x} = f'(z)\phi_1{}^o \\ \gamma_{yz} &= v_{,z} + w_{,y} = f'(z)\phi_2{}^o \end{aligned} \tag{4}$$

and, ε^o_x ε^o_y and γ^o_{xy} are reference surface strains and are defined as

$$\varepsilon^o_y = v^o_{,y},\ \varepsilon^o_x = u^o_{,x},\ \gamma^o_{xy} = u^o_{,y} + v^o_{,x} \tag{5}$$

The expression for different strain energies for the plate over the domain are given by

$$\begin{aligned} U^m = \frac{1}{2}\int_0^a\int_0^b \Bigg(& \begin{Bmatrix} \varepsilon^o_x \\ \varepsilon^o_y \\ \gamma^o_{xy} \end{Bmatrix}^T \begin{bmatrix} A_{11} & A_{12} & A_{16} \\ A_{12} & A_{22} & A_{26} \\ A_{16} & A_{26} & A_{66} \end{bmatrix} \begin{Bmatrix} \varepsilon^o_x \\ \varepsilon^o_y \\ \gamma^o_{xy} \end{Bmatrix} + \begin{Bmatrix} \varepsilon^o_x \\ \varepsilon^o_y \\ \gamma^o_{xy} \end{Bmatrix}^T \begin{bmatrix} B_{11} & B_{12} & B_{16} \\ B_{12} & B_{22} & B_{26} \\ B_{16} & B_{26} & B_{66} \end{bmatrix} \begin{Bmatrix} -w^o_{,xx} \\ -w^o_{,yy} \\ -2w^o_{xy} \end{Bmatrix} + \\ & \begin{Bmatrix} \varepsilon^o_x \\ \varepsilon^o_y \\ \gamma^o_{xy} \end{Bmatrix}^T \begin{bmatrix} C_{11} & C_{12} & C_{16} \\ C_{12} & C_{22} & C_{26} \\ C_{16} & C_{26} & C_{66} \end{bmatrix} \begin{Bmatrix} \phi^o_{1,x} \\ \phi^o_{2,y} \\ \phi^o_{1,y} + \phi^o_{2,x} \end{Bmatrix} \Bigg) dxdy \end{aligned} \tag{6}$$

$$U^b = \frac{1}{2}\int_0^a\int_0^b \left(\begin{Bmatrix} -w^o_{,xx} \\ -w^o_{,yy} \\ -2w^o_{xy} \end{Bmatrix}^T \begin{bmatrix} B_{11}\ B_{12}\ B_{16} \\ B_{12}\ B_{22}\ B_{26} \\ B_{16}\ B_{26}\ B_{66} \end{bmatrix} \begin{Bmatrix} \varepsilon^o_x \\ \varepsilon^o_y \\ \gamma^o_{xy} \end{Bmatrix} + \begin{Bmatrix} -w^o_{,xx} \\ -w^o_{,yy} \\ -2w^o_{xy} \end{Bmatrix}^T \begin{bmatrix} D_{11}\ D_{12}\ D_{16} \\ D_{12}\ D_{22}\ D_{26} \\ D_{16}\ D_{26}\ D_{66} \end{bmatrix} \begin{Bmatrix} -w^o_{,xx} \\ -w^o_{,yy} \\ -2w^o_{xy} \end{Bmatrix} + \begin{Bmatrix} -w^o_{,xx} \\ -w^o_{,yy} \\ -2w^o_{xy} \end{Bmatrix}^T \begin{bmatrix} E_{11}\ E_{12}\ E_{16} \\ E_{12}\ E_{22}\ E_{26} \\ E_{16}\ E_{26}\ E_{66} \end{bmatrix} \begin{Bmatrix} \phi^o_{1,x} \\ \phi^o_{2,y} \\ \phi^o_{1,y} + \phi^o_{2,x} \end{Bmatrix} \right) dxdy \tag{7}$$

$$U^{ab} = \frac{1}{2}\int_0^a\int_0^b \left(\begin{Bmatrix} \phi^o_{1,x} \\ \phi^o_{2,y} \\ \phi^o_{1,y} + \phi^o_{2,x} \end{Bmatrix}^T \begin{bmatrix} C_{11}\ C_{12}\ C_{16} \\ C_{12}\ C_{22}\ C_{26} \\ C_{16}\ C_{26}\ C_{66} \end{bmatrix} \begin{Bmatrix} \varepsilon^o_x \\ \varepsilon^o_y \\ \gamma^o_{xy} \end{Bmatrix} + \begin{Bmatrix} \phi^o_{1,x} \\ \phi^o_{2,y} \\ \phi^o_{1,y} + \phi^o_{2,x} \end{Bmatrix}^T \begin{bmatrix} E_{11}\ E_{12}\ E_{16} \\ E_{12}\ E_{22}\ E_{26} \\ E_{16}\ E_{26}\ E_{66} \end{bmatrix} \begin{Bmatrix} -w^o_{,xx} \\ -w^o_{,yy} \\ -2w^o_{xy} \end{Bmatrix} + \begin{Bmatrix} \phi^o_{1,x} \\ \phi^o_{2,y} \\ \phi^o_{1,y} + \phi^o_{2,x} \end{Bmatrix}^T \begin{bmatrix} F_{11}\ F_{12}\ F_{16} \\ F_{12}\ F_{22}\ F_{26} \\ F_{16}\ F_{26}\ F_{66} \end{bmatrix} \begin{Bmatrix} \phi^o_{1,x} \\ \phi^o_{2,y} \\ \phi^o_{1,y} + \phi^o_{2,x} \end{Bmatrix} \right) dxdy \tag{8}$$

$$U^s = \frac{1}{2}\int_0^a\int_0^b \left(\begin{Bmatrix} \phi^o_2 \\ \phi^o_1 \end{Bmatrix}^T \begin{bmatrix} H_{44} & H_{45} \\ H_{45} & H_{55} \end{bmatrix} \begin{Bmatrix} \phi^o_2 \\ \phi^o_1 \end{Bmatrix} \right) dxdy \tag{9}$$

where U^m, U^b, U^{ab} and U^S are membrane energy, bending energy, additional bending energy due to additional change in curvature and shear energy due to shear deformation respectively. The total Strain energy

$$U = U^m + U^b + U^{ab} + U^s \tag{10}$$

The expression for the potential of the external load

$$V = -\frac{1}{2}\int_0^a\int_0^b \left(\begin{Bmatrix} \dfrac{\partial w^0}{\partial x} \\ \dfrac{\partial w^0}{\partial y} \end{Bmatrix}^T \begin{bmatrix} N_{xx} & N_{xy} \\ N_{xy} & N_{yy} \end{bmatrix} \begin{Bmatrix} \dfrac{\partial w^0}{\partial x} \\ \dfrac{\partial w^0}{\partial y} \end{Bmatrix} \right) dxdy \tag{11}$$

where, N_{xx}, N_{yy} and N_{xy} are the in-plane loads in the x-direction, y-direction and in-plane shearing loads respectively. Kinetic energy expression may be expressed as

$$T_E = \frac{1}{2}\int_0^a\int_0^b \left(\begin{Bmatrix} \frac{\partial u^0}{\partial t} \\ \frac{\partial v^0}{\partial t} \\ \frac{\partial w^0}{\partial t} \\ \frac{\partial \phi_2^0}{\partial t} \\ \frac{\partial \phi_1^0}{\partial t} \end{Bmatrix}^T \begin{bmatrix} \rho h & 0 & 0 & 0 & 0 \\ 0 & \rho h & 0 & 0 & 0 \\ 0 & 0 & \rho h & 0 & 0 \\ 0 & 0 & 0 & \frac{\rho h^3}{12} & 0 \\ 0 & 0 & 0 & 0 & \frac{\rho h^3}{12} \end{bmatrix} \begin{Bmatrix} \frac{\partial u^0}{\partial t} \\ \frac{\partial v^0}{\partial t} \\ \frac{\partial w^0}{\partial t} \\ \frac{\partial \phi_2^0}{\partial t} \\ \frac{\partial \phi_1^0}{\partial t} \end{Bmatrix}\right) dxdy \tag{12}$$

In the above formulation, plate stiffness A_{ij}, B_{ij}, C_{ij}, D_{ij}, E_{ij}, F_{ij} and H_{ij} are defined as

$$(A_{ij}, B_{ij}, D_{ij}) = \int_{-h/2}^{h/2} \overline{Q}_{ij}(1, z, z^2)dz = \sum_{k=1}^{N} \int_{z_{k-1}}^{z_k} \overline{Q}_{ij}(1, z, z^2)dz \qquad (i, j = 1,2,6)$$

$$(C_{ij}, E_{ij}, F_{ij}) = \int_{-h/2}^{h/2} \overline{Q}_{ij}(1, z, f(z))f(z)dz = \sum_{k=1}^{N} \int_{z_{k-1}}^{z_k} \overline{Q}_{ij}(1, z, f(z))f(z)dz \ (i, j = 1,2,6) \tag{13}$$

$$H_{ij} = \int_{-h/2}^{h/2} \overline{Q}_{ij} f'(z)f'(z)dz = \sum_{k=1}^{N} \int_{z_k}^{z_{k-1}} \overline{Q}_{ij} f'(z)f'(z)dz \qquad (i, j = 4,5)$$

where, N is the number of orthotropic layer and $\overline{Q}_{ij}$ is the transformed elastic constants of the layer. U^m, U^b, U^{ab}, U^S, V and T of the symmetric laminated composite skew plate over the domain in oblique co-ordinate system (non-orthogonal) are obtained by transformation relation and are represented as U^{*m}, U^{*b}, U^{*ab}, U^{*S}, V^* and T^*

$$U^{*m} = \frac{1}{2}\int_0^1\int_0^1 f_1(u^o_{,\xi}, u^o_{,\eta}, v^o_{,\xi}, v^o_{,\eta}) \cos\psi \, d\xi \, d\eta \tag{14a}$$

$$U^{*b} = \frac{1}{2}\int_0^1\int_0^1 f_2(w^o_{,\xi\xi}, w^o_{,\xi\eta}, w^o_{,\eta\eta}, \phi^o_{1,\xi}, \phi^o_{1,\eta}, \phi^o_{2,\xi}, \phi^o_{2,\eta}) \cos\psi \, d\xi \, d\eta \tag{14b}$$

$$U^{*ab} = \frac{1}{2}\int_0^1\int_0^1 f_3(w^o_{,\xi\xi}, w^o_{,\xi\eta}, w^o_{,\eta\eta}, \phi^o_{1,\xi}, \phi^o_{1,\eta}, \phi^o_{2,\xi}, \phi^o_{2,\eta}) \cos\psi \, d\xi \, d\eta \tag{14c}$$

$$U^{*s} = \frac{1}{2}\int_0^1\int_0^1 f_4(\phi^o_1, \phi^o_2) \cos\psi \, d\xi \, d\eta \tag{14d}$$

$$V^* = -\frac{1}{2}\int_0^1\int_0^1 f_5(n_{xx}, n_{xy}, n_{yy}, w^o_{,\xi}, w^o_{,\eta}) \cos\psi \, d\xi \, d\eta \tag{14e}$$

$$T^* = \frac{1}{2}\int_0^1\int_0^1 f_6(u^o, v^o, w^o, \phi_1^o, \phi_2^o)\cos\psi\, d\xi\, d\eta \tag{14f}$$

The expressions for f_i (i=1,2,…6) are given in Appendix A

2.1 Plate prebuckling analysis

In the present investigation, parabolically and linearly varying in-plane compressive dynamic edge loadings are considered (See Figs. 1(a) and 1(b)). In the case of linearly varying in-plane edge loading, the stress distribution within the skew plate coincides with the applied edge load i.e. stress distribution within the skew plate is uniform. However, for parabolic edge loading, the stress distribution within the skew plate is not uniform. In the case of parabolic in-plane load, initially the static component (N_s) of the in-plane loading is applied at the plate edge and stress fields within the skew plate are obtained by solving the plate membrane problem. The in-plane stress distributions are assumed to be uniform across the entire thickness. The correct stress distribution within the skew plate is the one which minimizes the membrane strain energy of the plate and satisfies the boundary condition of the problem. The membrane strain energy (V^m) of a plate of thickness 'h' of composite skew plate is given by

$$V^m = \frac{h}{2}\iint_A \begin{Bmatrix} n_{\xi\xi} \\ n_{\eta\eta} \\ n_{\xi\eta} \end{Bmatrix} \begin{bmatrix} A_{11}^* & A_{12}^* & A_{16}^* \\ A_{12}^* & A_{22}^* & A_{26}^* \\ A_{16}^* & A_{26}^* & A_{66}^* \end{bmatrix}^{-1} \begin{Bmatrix} n_{\xi\xi} \\ n_{\eta\eta} \\ n_{\xi\eta} \end{Bmatrix} cos\psi d\xi d\eta \tag{15}$$

$$\text{where, } n_{\xi\xi} = \frac{\partial^2 \Phi}{\partial \eta^2}, \quad n_{\eta\eta} = \frac{\partial^2 \Phi}{\partial \xi^2}, \quad n_{\xi\eta} = -\frac{\partial^2 \Phi}{\partial \xi \partial \eta}, \quad A_{ij} = \int_{-h/2}^{h/2} \overline{Q}_{ij} dz = \sum_{k=1}^{N} \int_{z_{k-1}}^{z_k} \overline{Q}_{ij} dz \tag{16}$$

where Q_{ij} is the transformed reduced stiffness, Φ is the stress function and [A^*] is the extensional laminate stiffness in oblique co-ordinate system. The relationship between extensional laminate stiffness in oblique co-ordinate system and in Cartesian co-ordinate system is

$$[A^*] = [T^r]^{-T}[A][T^r]^{-1} \tag{17}$$

Where the transformation matrix [T^Y] is

$$T^r = \begin{bmatrix} 1 & 0 & 0 \\ \sin^2\psi & \cos^2\psi & \sin\psi\cos\psi \\ 2\sin\psi & 0 & \cos\psi \end{bmatrix} \tag{18}$$

Following Timoshenko and Goodier (1960), Ritz method is adopted to minimize the membrane strain energy of the skew plate in this study. The boundary conditions of the plate membrane problem are given here for parabolically varying uniaxial in-plane edge load (see Fig. 1(a))

$$\begin{aligned} &\xi = 0, b \quad \overline{N}_{\xi\eta} = 0; \ \overline{N}_{\xi\xi} = 4N_0 \frac{\eta}{b}(1 - \frac{\eta}{b}) \\ &\eta = 0, b \quad \overline{N}_{\xi\eta} = 0; \ \overline{N}_{\eta\eta} = 0 \end{aligned} \tag{19}$$

Table 1 All six constants of three layered [0/90/0] composite skew plate (ψ=30°, *a/b*=1, *a/h* =100)

Types of In-plane Loading	α_1	α_2	α_3	α_4	α_5	α_6
Parabolic Load	0.188	1.327	-0.103	-0.025	-2.603	1.404
Linearly Varying Load	0	0	0	0	0	0

The stress function is assumed in the form of a series as

$$\Phi = \Phi_0 + \alpha_1\Phi_1 + \alpha_2\Phi_2 + \alpha_3\Phi_3 + \alpha_4\Phi_4 + \alpha_5\Phi_5 + \alpha_6\Phi_6 \ldots \tag{20}$$

where, α_i (i=1,2,...6) are constants to be determined such that the membrane strain energy is minimized and boundary conditions are satisfied. In the present investigation, six terms are considered in Eq. (20) for accurate result. The stress function for the parabolic in-plane edge loading is assumed as

$$\Phi = 2N_0\frac{\eta^2}{3}\left(\frac{\eta}{b}-\frac{\eta^2}{2b^2}\right)+(\xi^2-a\xi)^2(\eta^2-\eta b)^2(\alpha_1+\alpha_2\xi+\alpha_3\eta+\alpha_4\xi^2+\alpha_5\xi\eta+\alpha_6\eta^2) \tag{21}$$

Substituting the Eqs. (21) and (16) in Eq. (15) and carrying out integration, an expression in second degree in α_i (i = 1,2,…6) are obtained. The constants α_i (i = 1,2,…6) are evaluated from the algebraic equations by minimizing membrane strain energy (V^m) Constants are tabulated in Table 1 for a three layered [0/90/0] composite skew plate for parabolic in-plane loading

2.2 Derivation of orthogonal polynomial

Consider a skew plate with length '*a*', breadth '*b*' and thickness '*h*'. The skew plate domain in the *x-y* plane is transformed into unit square plate domain in ξ-η plane, by using the following transformation equation

$$x = a\xi + b\eta\sin\psi;\ y = b\eta\cos\psi \tag{22}$$

The following transformation rule is used to map any function of functional from *x-y* plane to ξ-η plane.

$$\begin{bmatrix}\frac{\partial}{\partial x}\\ \frac{\partial}{\partial y}\end{bmatrix}=\begin{bmatrix}\frac{1}{a} & 0\\ -\frac{\tan\psi}{a} & \frac{\sec\psi}{b}\end{bmatrix}\begin{bmatrix}\frac{\partial}{\partial\xi}\\ \frac{\partial}{\partial\eta}\end{bmatrix} \tag{23}$$

$$\begin{bmatrix}\frac{\partial^2}{\partial x^2}\\ \frac{\partial^2}{\partial y^2}\\ \frac{\partial^2}{\partial x\partial y}\end{bmatrix}=\begin{bmatrix}\frac{1}{a^2} & 0 & 0\\ \frac{\tan^2\psi}{a^2} & \frac{\sec^2\psi}{b^2} & -\frac{2\tan\psi\sec\psi}{ab}\\ -\frac{\tan\psi}{a^2} & 0 & \frac{\sec\psi}{ab}\end{bmatrix}\begin{bmatrix}\frac{\partial^2}{\partial\xi^2}\\ \frac{\partial^2}{\partial\eta^2}\\ \frac{\partial^2}{\partial\xi\partial\eta}\end{bmatrix} \tag{24}$$

To generate orthogonal polynomials satisfying essential boundary conditions over the unit

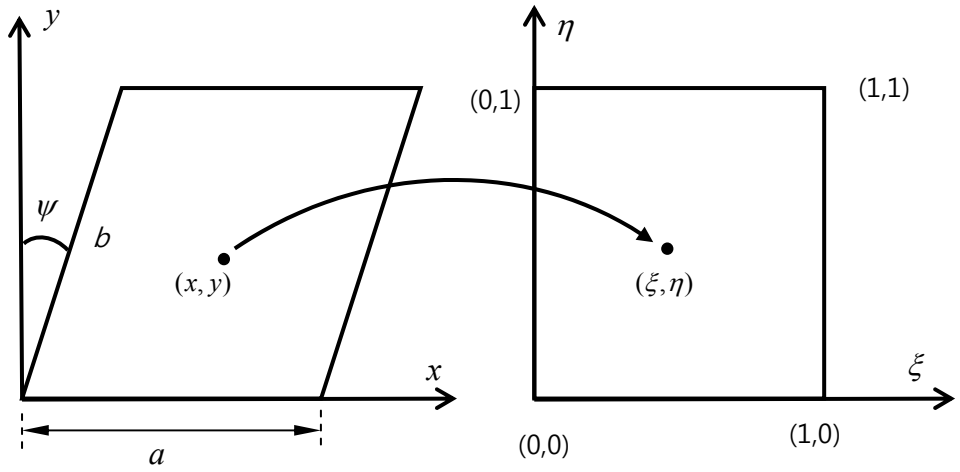

Fig. 2 Mapping of the skew plate domain into a unit square plate domain

square plate domain in ξ-η plane, following displacement fields are used

$$\begin{aligned}
\tilde{u}^o(\xi,\eta,t) &= \sum_{j=1}^{\Upsilon} U_j(t)\hat{\alpha}_j(\xi,\eta)\\
\tilde{v}^o(\xi,\eta,t) &= \sum_{j=1}^{\Upsilon} V_j(t)\hat{\beta}_j(\xi,\eta)\\
\tilde{w}^o(\xi,\eta,t) &= \sum_{j=1}^{\Upsilon} W_j(t)\hat{\phi}_j(\xi,\eta)\\
\tilde{\phi}_1^{\,o}(\xi,\eta,t) &= \sum_{j=1}^{\Upsilon} K_j(t)\hat{\gamma}_j(\xi,\eta)\\
\tilde{\phi}_2^{\,o}(\xi,\eta,t) &= \sum_{j=1}^{\Upsilon} L_j(t)\hat{\delta}_j(\xi,\eta)
\end{aligned} \tag{25}$$

where Υ is the order of approximation to get the desired accuracy, U_j, V_j, W_j, K_j and $L_j$are unknowns and $\hat{\alpha}_j,\hat{\beta}_j,\hat{\phi}_j,\hat{\gamma}_j$ and $\hat{\delta}_j$ are boundary characteristics orthonormal polynomial functions which are generated on the standard square domain using the Gram-Schmidt process. Orthonormal polynomials $\hat{\phi}_j(\xi,\eta)$ over the region $0\leq\xi\leq1$, $0\leq\eta\leq1$ have been generated using linearly independent set of functions $F_j=f^*f_j$, j=1,2,3..., with

$$f = \xi^p(1-\xi)^q\eta^r(1-\eta)^s \tag{26a}$$

$$f_j = \left\{1,\xi,\eta,\xi^2,\xi\eta,\eta^2,\xi^3,\xi^2\eta,\xi\eta^2,\eta^3,...\right\} \tag{26b}$$

The value of 'p' depends on the boundary condition on ξ=0, 1. At ξ=0, p=0, 1, 2 respectively for free, simply supported and clamped boundary condition. At ξ=1, q=0, 1, 2 respectively for free, simply supported and clamped boundary condition. In similar way, the value of r and s are chosen

for η=0, 1.

$$\phi_1 = F_1, \quad \phi_j = F_j - \sum_{i=1}^{j-1} \alpha_{ji}\phi_i, \tag{27}$$

$$\alpha_{ji} = \frac{< F_j, \phi_i >}{< \phi_i, \phi_i >}, \quad i = 1,\ 2,\ 3,\ \ldots,(j-1), \quad j = 2, 3, 4, \ldots, N \tag{28}$$

The inner product of the functions ϕ_i and ϕ_j can be defined as

$$< \phi_i, \phi_j >= \int_0^1 \int_0^1 \phi_i(\xi,\eta)\phi_j(\xi,\eta)\, d\xi d\eta \tag{29}$$

The norm of the function ϕ_j is given by

$$\left\| \phi_j \right\| = < \phi_j, \phi_j >^{1/2} = \left[\int_0^1 \int_0^1 \phi_j(\xi,\eta)\phi_j(\xi,\eta)\, d\xi d\eta \right]^{1/2} \tag{30}$$

The normalization has been done by

$$\hat{\phi}_j = \frac{\phi_j}{\left\| \phi_j \right\|} \tag{31}$$

The total potential energy function $\prod(U+V)$ and kinetic energy (T_E) are transformed from *x*-*y* plane to ξ-η plane by using Eq. (23) and (24) Further, the orthonormal polynomial functions are substituted to get the energy function in ξ-η plane. The total potential energy and kinetic energy expression involves with different unknowns U_j, V_j, W_j, K_j and L_j. Rayleigh-Ritz method is used as follows to determine governing eigen value equation and are represented as

$$\sum [K - \lambda M] \begin{Bmatrix} \{u\} \\ \{v\} \\ \{w\} \\ \{k\} \\ \{l\} \end{Bmatrix} = \{0\} \tag{32}$$

$$\{u\} = \begin{Bmatrix} U_1 \\ U_2 \\ . \\ . \\ . \\ U_\Upsilon \end{Bmatrix}, \{v\} = \begin{Bmatrix} V_1 \\ V_2 \\ . \\ . \\ . \\ V_\Upsilon \end{Bmatrix}, \{w\} = \begin{Bmatrix} W_1 \\ W_2 \\ . \\ . \\ . \\ W_\Upsilon \end{Bmatrix}, \{k\} = \begin{Bmatrix} K_1 \\ K_2 \\ . \\ . \\ . \\ K_\Upsilon \end{Bmatrix}, \{l\} = \begin{Bmatrix} L_1 \\ L_2 \\ . \\ . \\ . \\ L_\Upsilon \end{Bmatrix} \tag{33}$$

The Eq. (32) constitutes a set of 5Υ simultaneous homogeneous algebraic equation called Galerkin's equation and also referred as Ritz system.

2.3 Instability analysis of Mathieu equation

The dynamic instability of the plate loaded by periodic uniform in-plane load $N_{xx}=N_s+N_t \cos pt$ analysed. The dynamic in-plane load has both static component (N_s) and dynamic component (N_t). Using Rayleigh-Ritz method, the ordinary differential equations i.e., Mathieu equations describing the plate linear dynamic instability was derived as follows

$$[M]\{\ddot{\delta}\}+\left[[K_L]-(N_s+N_t\cos pt)[K_G]\right]\{\delta\}=\{0\} \tag{34}$$

where $[M]$, $[K_L]$ and $[K_G]$ are respectively the mass, linear and geometric stiffness matrices. In Eq. (34), the static and dynamic components are expressed as

$$N_s=\alpha N_{cr} \text{ and } N_t=\beta N_{cr} \tag{35}$$

where α and β are static and dynamic load factors respectively and N_{cr} is the static buckling load. The Eq. (34) is a second order differential equation with periodic coefficients. The critical buckling load is evaluated from the solution of linear eigen value problem by neglecting the mass, non-linear stiffness and time dependant load terms. Similarly the solutions of the eigen value problem associated with the differential equation neglecting terms containing N_s and N_t gives the natural frequencies. On the boundaries of the region of instability the differential equation system has periodic solution with period T or $2T$. Two solutions with same period confine the region of instability and two solutions with different period confine the region of stability (Bolotin 1964). The solution of the Eq. (34) with period T and $2T$, respectively, are assumed in the form of Fourier series as

$$\delta(t)=b_0+\sum_{k=2,4,6}^{\infty}\left(a_k\sin\frac{kpt}{2}+b_k\cos\frac{kpt}{2}\right) \tag{36a}$$

$$\delta(t)=\sum_{k=1,3,5}^{\infty}\left(a_k\sin\frac{kpt}{2}+b_k\cos\frac{kpt}{2}\right) \tag{36b}$$

where a_k and b_k are arbitrary constants. Substituting Eq. (36a) or (36b) into Eq. (34) and equating the coefficients of identical $\sin\frac{kpt}{2}$ and $\cos\frac{kpt}{2}$ leads to a system of homogeneous algebraic equations in a_k and b_k. For a nontrivial solution the determinant of the coefficient matrix of a_k and b_k must vanish. The size of the above determinant is infinite as we have assumed the solution in the form of infinite series. The determinants are shown to be belonging to a class of converging determinant known as normal determinant (Bolotin 1964). The first order (from Eq. (37)) and second order (from Eq. (38)) approximation to boundaries of first regions of instability corresponding to period $2T$ is obtained by solving following two eigen value problems respectively.

$$\left|K^*\pm 0.5\beta N_{cr}K_G-0.25Mp_1^2\right|=0 \tag{37}$$

$$\begin{vmatrix} K^*\pm 0.5\beta N_{cr}K_G & -0.5\beta N_{cr}K_G \\ -0.5\beta N_{cr}K_G & K^*-2.25Mp_1^2 \end{vmatrix}-p_2^2\begin{vmatrix} 0.25M & 0 \\ 0 & 0 \end{vmatrix}=0 \tag{38}$$

Second region of instability with first order approximation (from Eqs. (39) and (40)) and second order approximation (from Eqs. (41) and (42)) corresponding to period T are determined from

$$\left|K^* - Mp_1^2\right| = 0 \tag{39}$$

$$\begin{vmatrix} K^* & -0.5\beta N_{cr}K_G \\ -\beta N_{cr}K_G & K^* \end{vmatrix} - p_1^2 \begin{vmatrix} 0 & 0 \\ 0 & M \end{vmatrix} = 0 \tag{40}$$

$$\begin{vmatrix} K^* & -0.5\beta N_{cr}K_G \\ -0.5\beta N_{cr}K_G & K^* - 4Mp_1^2 \end{vmatrix} - p_2^2 \begin{vmatrix} M & 0 \\ 0 & 0 \end{vmatrix} = 0 \tag{41}$$

$$\begin{vmatrix} K^* & -0.5\beta N_{cr}K_G & 0 \\ -\beta N_{cr}K_G & K^* & -0.5\beta N_{cr}K_G \\ 0 & -0.5\beta N_{cr}K_G & K^* - 4Mp_1^2 \end{vmatrix} - p_2^2 \begin{vmatrix} 0 & 0 & 0 \\ 0 & M & 0 \\ 0 & 0 & 0 \end{vmatrix} = 0 \tag{42}$$

Third region of instability (from Eq. (43) and (44)) and fourth region instability (from Eq. (45) and (46)) corresponding to period T and $2T$ are determined from,

$$\begin{vmatrix} K^* + 0.5\beta N_{cr}K_G - 0.25Mp_3^2 & 0.5\beta N_{cr}K_G \\ 0.5\beta N_{cr}K_G & K^* - 2.25Mp_4^2 \end{vmatrix} = 0 \tag{43}$$

$$\begin{vmatrix} K^* - 0.5\beta N_{cr}K_G - 0.25Mp_3^2 & 0.5\beta N_{cr}K_G \\ 0.5\beta N_{cr}K_G & K^* - 2.25Mp_4^2 \end{vmatrix} = 0 \tag{44}$$

$$\begin{vmatrix} K^* - Mp_3^2 & 0.5\beta N_{cr}K_G & 0 \\ 0.5\beta N_{cr}K_G & K^* - 4Mp_1^2 & 0.5\beta N_{cr}K_G \\ 0 & 0.5\beta N_{cr}K_G & K^* - 9Mp_4^2 \end{vmatrix} = 0 \tag{45}$$

$$\begin{vmatrix} K^* & 0.5\beta N_{cr}K_G & 0 & 0 \\ \beta N_{cr}K_G & K^* - Mp_3^2 & 0.5\beta N_{cr}K_G & 0 \\ 0 & 0.5\beta N_{cr}K_G & K^* - 4Mp_3^2 & 0.5\beta N_{cr}K_G \\ 0 & 0 & 0.5\beta N_{cr}K_G & K^* - 9Mp_4^2 \end{vmatrix} = 0 \tag{46}$$

where, $K^*=[K]-N_S[K_G]$

Solving for p_4 from $(K^* - 2.25Mp_4^2)$ and substituting for p_3 of Eqs. (43) and (44) one can calculate third zone of instability of period $2T$. Similarly solving for p_4 from $(K^* - 9Mp_4^2)$ and substituting for p_3 of Eqs. (45) and (46) one can calculate fourth zone of instability of period T.

Table 2(a) Critical buckling coefficient (k_i) isotropic square skew plates (a/b=1, a/h=100) for different skew angles (ψ) under uniform in-plane loading

Type of Supports	Skew angle (ψ)	Dimensionless buckling coefficient (k_i)		
		Present solution	Wang (1997)	Babu and Kant (1999)
Simply supported plate (SSSS)	0°	4	4.0	4.0
	15°	3.826	3.824	3.830
	30°	3.323	3.316	3.330
	45°	2.559	2.525	2.557
			Durvasula (1970)	Wang *et al.* (1992)
Clamped supported plate (CCCC)	0°	10.074	10.074	10.074
	15°	9.431	9.462	9.479
	30°	7.612	7.638	7.734
	45°	5.110	5.110	5.172

Note: $k_i=N_{cr}b^2\cos^4\psi/\pi^2D$

Table 2(b) Critical buckling coefficients for isotropic and composite [0/90/0] square plate (a/b=1, a/h=100) under parabolic in-plane loading

Type of Supports	Buckling coefficients (k_i) for isotropic plate			Buckling coefficients (k_c) for composite [0/90/0] plate	
	Present	Wang *et al.* (2007)	Panda and Ramachandra (2010)	Present (Numerical)	Present (ABAQUS)
SSSS	5.24	5.24	5.24	27.50	27.51
SCSC	9.19	9.19	9.17	34.38	34.39
CSCS	9.05	9.05	9.03	93.93	93.63
CCCC	13.57	13.58	13.55	97.64	97.01

Note: $k_c=N_{cr}b^2/\pi^2E_{22}h^3$, A 8-noded doubly curved thick shell element is used in ABAQUS

3. Results and discussion

The buckling load obtained from present method of solution for skew plate subjected to uniform in-plane loading and for rectangular plate with non-uniform in-plane loading are compared well with open literature and given in Table 2(a) and Table 2(b), respectively.

The mechanical properties used in the present analysis for composite skew plate are: E_{11}/E_{22}=25, $G_{12}=G_{13}$=0.5 E_{22}, G_{23}= 0.2 E_{22} and ν_{12}=0.25. The dynamic instability regions are represented as a plot of dimensionless excitation frequency $\Omega\ (=\frac{pa^2}{\pi^2 h}\sqrt{\frac{\rho}{E_{22}}})$ for composite skew plate against dimensionless dynamic load factor (β). The principal dynamic instability regions of simply supported (SSSS) eight layered cross-ply [$(0/90/90/0)_s$] composite skew plate (a/b=1, a/h=100) with skew angle ψ=0° and 30° are obtained from the present method are compared with Noh and Lee (2014) and is shown in Fig. 3(a) and Fig. 3(b), respectively. It is observed from figure that the principal instability regions with first order approximation are compared well with reference instability regions.

Fig. 4 shows the first four instability zones of simply supported cross-ply [0/90/0] composite laminated skew plate (a/b=1, a/h=100, ψ=30°, α=0) under non-uniform (parabolic) in-plane

loading. The zone-I and zone- III instability zones correspond to period 2T, whereas, zone-II and zone- IV instability zones are for period T. It is reflected in the figure that for all the zones of instability, the width of instability increases with the increase of dynamic load factor. At a dynamic load factor (β) of 0.7, the widths (Δp) of instability are $1.1798\frac{\pi^2 h}{pa^2}\sqrt{\frac{E_{22}}{\rho}}$, $0.1981\frac{\pi^2 h}{pa^2}\sqrt{\frac{E_{22}}{\rho}}$, $0.0576\frac{\pi^2 h}{pa^2}\sqrt{\frac{E_{22}}{\rho}}$ and $0.0143\frac{\pi^2 h}{pa^2}\sqrt{\frac{E_{22}}{\rho}}$ for zone-I, zone-II, zone-III and zone-IV, respectively. At any particular value of dynamic load factor, the width (Δp) of the zone of instability is the maximum for zone-I (principal zone) and minimum for zone-IV. Principal zone has greater practical importance due to its maximum width of instability. The width of instability zone is slightly decreases for higher order approximation as shown in Fig. 4. At a dynamic load factor (β) of 0.7, the difference of width of instability between first order and second order for zone-I is $0.0324\frac{\pi^2 h}{pa^2}\sqrt{\frac{E_{22}}{\rho}}$ and for zone-II the difference of width is $0.0590\frac{\pi^2 h}{pa^2}\sqrt{\frac{E_{22}}{\rho}}$. The principal zone of instability with second-order approximation results are presented in subsequent figures as it is more practical and accurate.

The influence of skew angle on principal zone of instability of simply supported cross-ply [0/90/0] composite laminated skew plate (a/b=1, a/h=100, ψ=30°, α=0) under parabolic in-plane loading is presented in Fig. 5. At a dynamic load factor (β) of 0.7, the width of principal instability zones are, $1.0633\frac{\pi^2 h}{pa^2}\sqrt{\frac{E_{22}}{\rho}}$, $1.0853\frac{\pi^2 h}{pa^2}\sqrt{\frac{E_{22}}{\rho}}$, $1.1799\frac{\pi^2 h}{pa^2}\sqrt{\frac{E_{22}}{\rho}}$ and $1.4571\frac{\pi^2 h}{pa^2}\sqrt{\frac{E_{22}}{\rho}}$ for ψ=0°, 15°, 30° and 45°, respectively. It is observed that the skew plate becomes more unstable

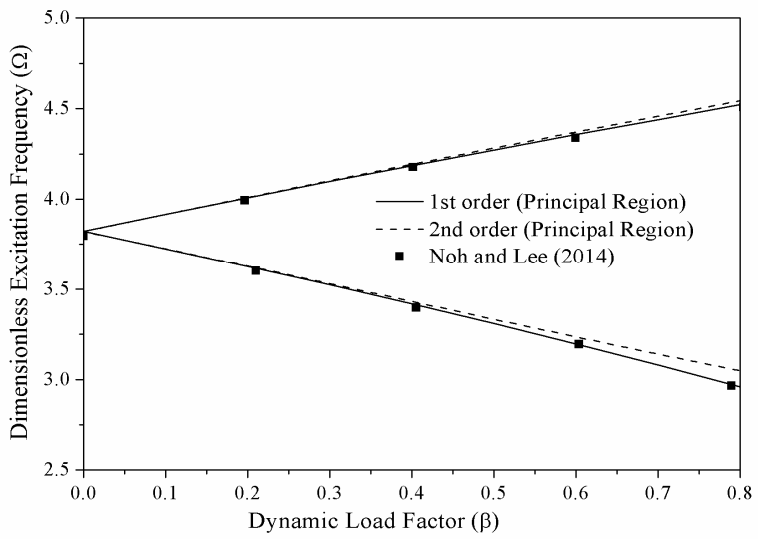

Fig. 3(a) Comparison of the principal instability region of a simply supported (SSSS) eight layered symmetric cross-ply [0/90/90/0/0/90/90/0] composite square plate (a/b=1, a/h=100, ψ=0°, α=0) subjected to uniform in-plane load

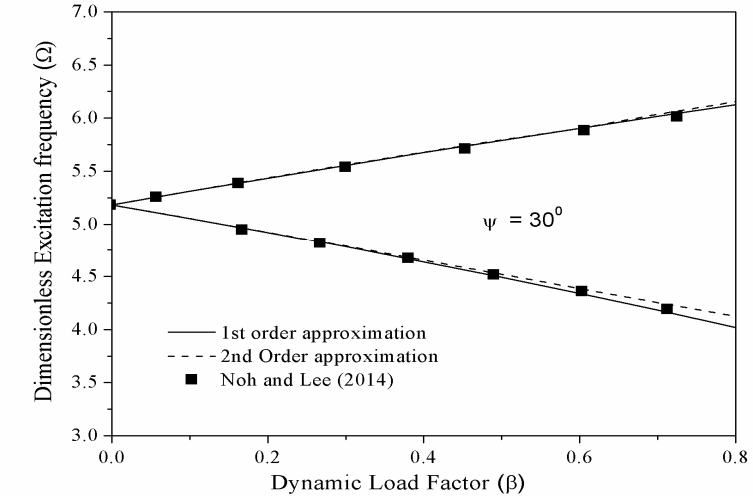

Fig. 3(b) Comparison of the principal instability region of a simply supported (SSSS) eight layered symmetric cross-ply [0/90/90/0/0/90/90/0] composite skew plate (a/b=1, a/h=100, ψ=30°, α=0) subjected to uniform in-plane load

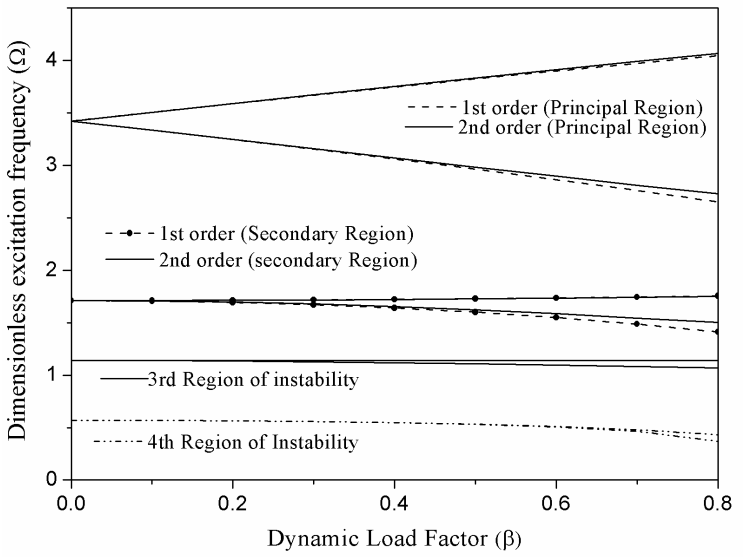

Fig. 4 Four instability zones of the SSSS three layered cross-ply [0/90/0] composite skew plates (a/b=1, a/h=100, ψ=30°, α=0) subjected to parabolic in-plane loading

as the skew angle increases.

The effect of shear deformation for a three layered cross-ply [0/90/0] composite skew plate (a/b=1, ψ=30°, α=0) subjected to uniform in-plane loading is studied in Fig. 6. The influence of shear deformation on frequency becomes pronounced when the ratio of side to thickness decreases, resulting lesser width of instability zone. The width of principal instability zones for above square composite skew plate (ψ=30°) decreases with increase of plate thickness as expected.

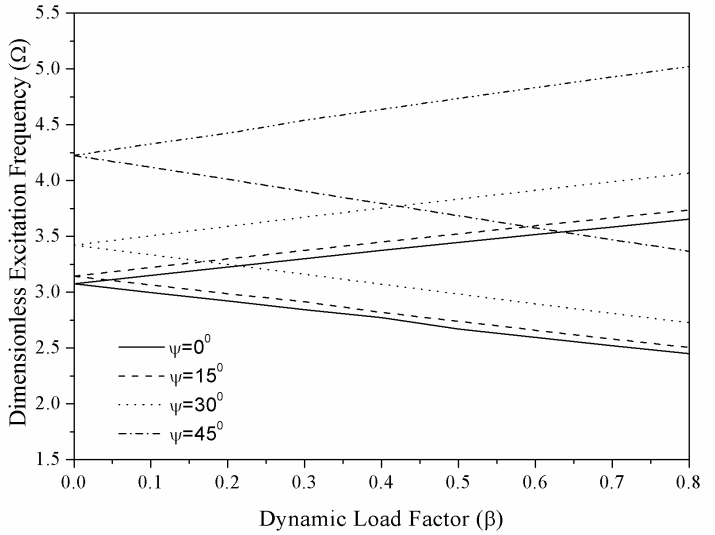

Fig. 5 Principal instability zones of the SSSS three layered cross-ply [0/90/0] composite skew plates (a/b=1, a/h=100, α=0) subjected to parabolic in-plane loading for different skew angle (ψ)

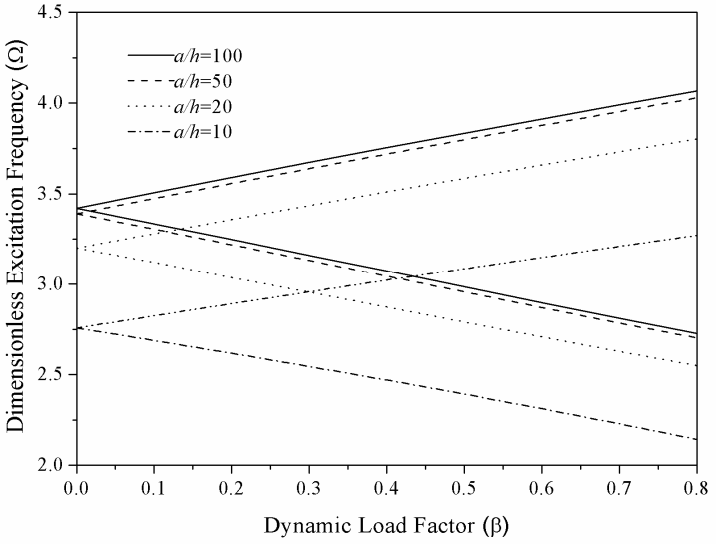

Fig. 6 Principal instability zones of the SSSS three layered cross-ply [0/90/0] composite skew plates (a/b=1, ψ=30°, α=0) subjected to parabolic in-plane loading for different span to thickness (a/h) ratio

At a dynamic load factor (β) of 0.7, the width of principal instability zones are, $1.1799\frac{\pi^2 h}{pa^2}\sqrt{\frac{E_{22}}{\rho}}$, $1.1691\ \frac{\pi^2 h}{pa^2}\sqrt{\frac{E_{22}}{\rho}}$, $1.1036\frac{\pi^2 h}{pa^2}\sqrt{\frac{E_{22}}{\rho}}$ and $0.9806\frac{\pi^2 h}{pa^2}\sqrt{\frac{E_{22}}{\rho}}$ for side to thickness ratio a/h= 100, 50, 20 and 10, respectively

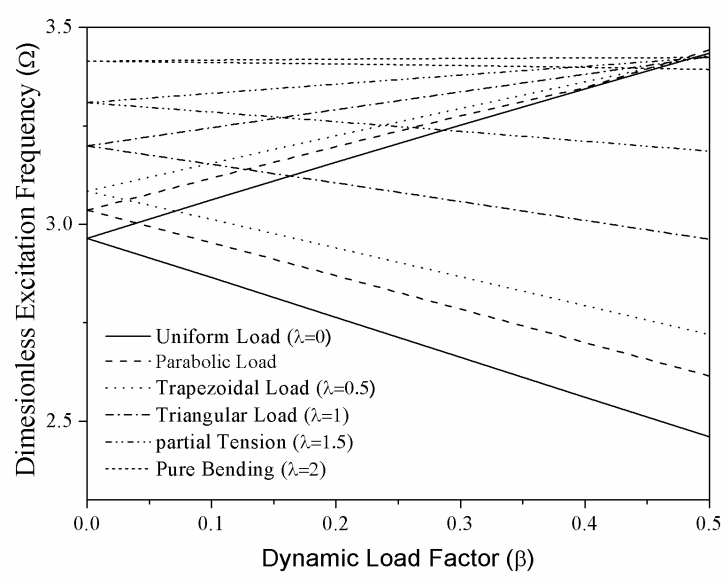

Fig. 7 Principal instability zones of SSSS three layered cross-ply [0/90/0] composite skew plates (a/b=1, a/h=100, ψ=30°, α=0.25) for parabolic and different types of linearly varying in-plane loadings

Fig. 7 represents the behaviour of three layered cross-ply [0/90/0] composite skew plate (a/b=1, a/h=100, ψ=30°, α=0.25) for different linearly varying in-plane loads. The linearly varying in-plane loads are denoted by $N_s = \alpha N_{cr}(1-\lambda(\frac{\eta}{b}))$ and $N_t = \beta N_{cr}(1-\lambda(\frac{\eta}{b}))$ where αN_{cr} and βN_{cr} are the intensity of static and dynamic components of compressive load at the edge y=0. By taking various values of λ, we obtain different in-plane load distribution: uniform (λ=0), trapezoidal (λ=0.5), triangular (λ=1), partial tension (λ=1.5) and pure bending (λ=2.0). The principal instability zones for the composite skew plate (a/b=1, a/h=100, ψ=30°, α=0.2) subjected to time dependent linearly varying in-plane loads with λ=0, 0.5, 1, 1.5 and 2.0 are represented as a plot of dimensionless excitation frequency $\frac{\pi^2 h}{pa^2}\sqrt{\frac{E_{22}}{\rho}}$ against dimensionless dynamic load factor (β) of uniform loading. It is observed that the width of the dynamic instability region is the maximum for the uniform in-plane load and minimum for the pure bending case. This is because of the buckling load is minimum for uniform loaded panel and maximum for pure in-plane bending case. The width of the primary instability zones are, $0.9747\frac{\pi^2 h}{pa^2}\sqrt{\frac{E_{22}}{\rho}}$, $0.7097\frac{\pi^2 h}{pa^2}\sqrt{\frac{E_{22}}{\rho}}$, $0.4640\frac{\pi^2 h}{pa^2}\sqrt{\frac{E_{22}}{\rho}}$, $0.2381\frac{\pi^2 h}{pa^2}\sqrt{\frac{E_{22}}{\rho}}$ and $0.03\frac{\pi^2 h}{pa^2}\sqrt{\frac{E_{22}}{\rho}}$ for λ=0, 0.5, 1, 1.5 and 2.0, respectively for dynamic load factor of 0.5 (note that the dynamic load factor corresponding to that of uniform loading). The width of the primary instability zones for parabolic loading is $0.8278\frac{\pi^2 h}{pa^2}\sqrt{\frac{E_{22}}{\rho}}$.

The influence of aspect ratio (a/b) on principal instability zones of three layered cross-ply

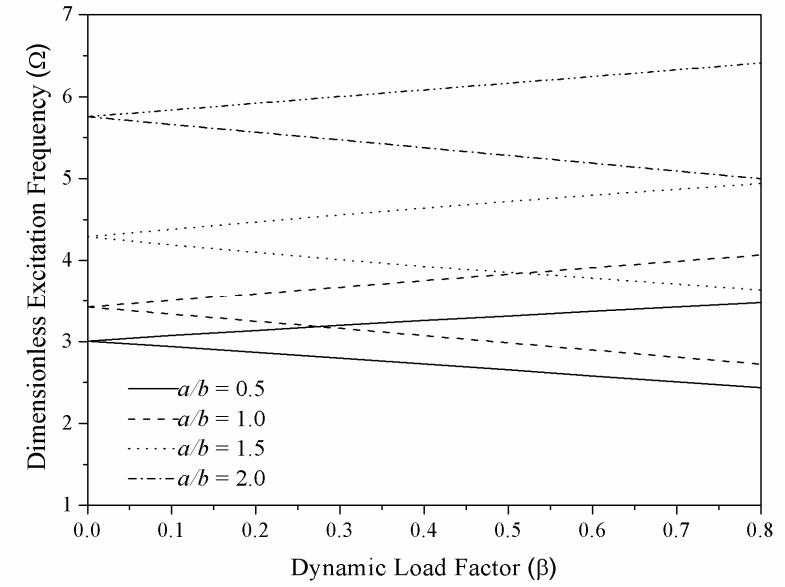

Fig. 8 Principal instability zones of SSSS three layered cross-ply [0/90/0] composite skew plates (a/h=100, ψ=30°, α=0) subjected to parabolic in-plane loading for different aspect (a/b) ratio

[0/90/0] composite skew plate (a/b=1, a/h=100, ψ=30°, α=0) subjected to uniform in-plane loading is shown in Fig. 8. In the present analysis, '*a*' is kept constant and '*b*' is varied. At a dynamic load factor (β) of 0.7, the width of principal instability zones are, $2.126\frac{\pi^2 h}{pa^2}\sqrt{\frac{E_{22}}{\rho}}$, $1.5123\frac{\pi^2 h}{pa^2}\sqrt{\frac{E_{22}}{\rho}}$, $1.1799\frac{\pi^2 h}{pa^2}\sqrt{\frac{E_{22}}{\rho}}$ and $0.9147\frac{\pi^2 h}{pa^2}\sqrt{\frac{E_{22}}{\rho}}$ for a/b=2, 1.5, 1, and 0.5, respectively. It shows that as the aspect ratio (a/b) increases i.e., for the slender plate the width of instability region increase as expected.

The edge restraint has a significant effect on principal instability zones of three layered cross-ply [0/90/0] composite skew plate (a/b=1, a/h=100, ψ=30°, α=0) subjected to parabolic in-plane loading and it is presented in Fig. 9. In the present analysis, four different boundary conditions considered as follows: all edges simply supported (SSSS), loaded edges simply supported and other two edges clamped (SCSC), loaded edges clamped and other two edges simply supported (CSCS) and all edges clamped (CCCC). At a dynamic load factor (β) of 0.7, the width of the primary instability zones are, $1.1799\frac{\pi^2 h}{pa^2}\sqrt{\frac{E_{22}}{\rho}}$, $1.0280\frac{\pi^2 h}{pa^2}\sqrt{\frac{E_{22}}{\rho}}$, $0.7417\frac{\pi^2 h}{pa^2}\sqrt{\frac{E_{22}}{\rho}}$ and $0.7333\frac{\pi^2 h}{pa^2}\sqrt{\frac{E_{22}}{\rho}}$ for SSSS, SCSC, CSCS and CCCC boundary conditions, respectively. Here, it is noted that more the edge restraint narrower is the width of zone of instability. Static in-plane parabolic load has also the influence on the width of principal instability zones of a three layered cross-ply [0/90/0] composite skew plate (a/b=1, a/h=100, ψ=30°) and has been shown in Fig. 10.

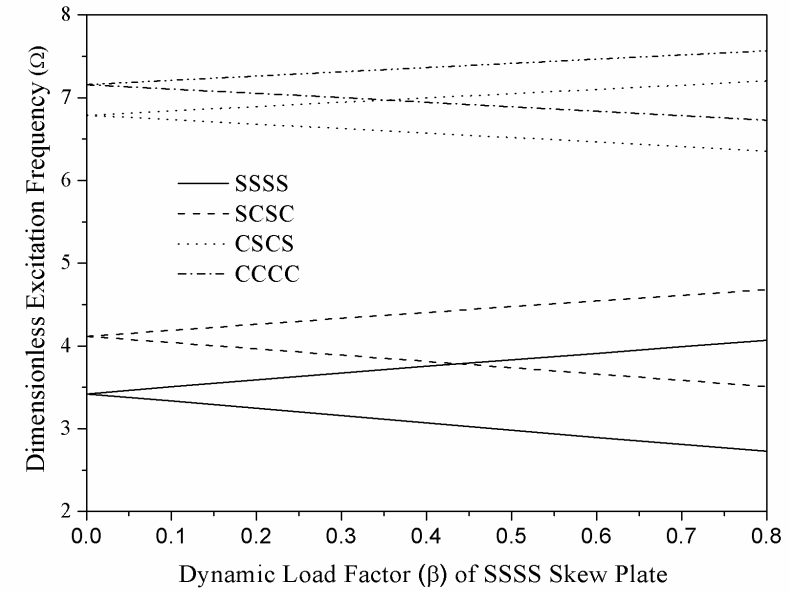

Fig. 9 Principal instability zones of three layered cross-ply [0/90/0] composite skew plates (a/b=1, a/h=100, ψ=30°, α=0) subjected to parabolic in-plane loading for different boundary conditions

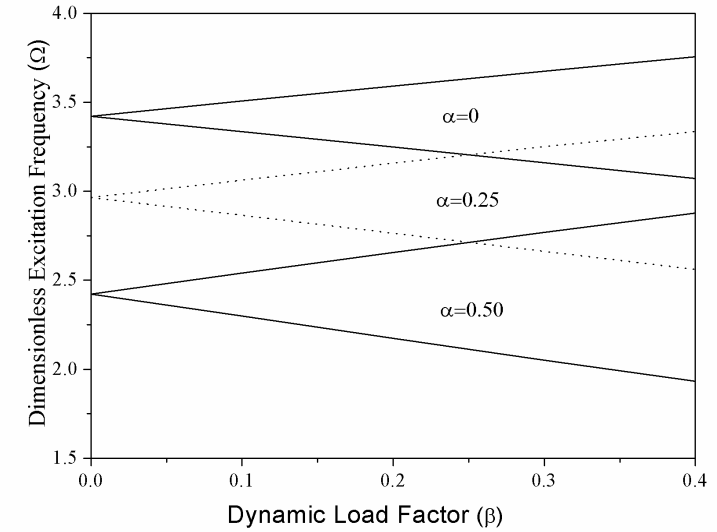

Fig. 10 Principal instability zones of SSSS three layered cross-ply [0/90/0] composite skew plates (a/b=1, a/h=100, ψ=30°) subjected to parabolic in-plane loading for different static load factor (α)

For a dynamic load factor (β) of 0.4, the width of the primary instability zones are, 0.6816 $\frac{\pi^2 h}{pa^2}\sqrt{\frac{E_{22}}{\rho}}$, 0.7741 $\frac{\pi^2 h}{pa^2}\sqrt{\frac{E_{22}}{\rho}}$ and 0.9456 $\frac{\pi^2 h}{pa^2}\sqrt{\frac{E_{22}}{\rho}}$ for static load factor α=0, 0.25 and 0.5, respectively. It is concluded that the width of principal instability zone increases with increase of

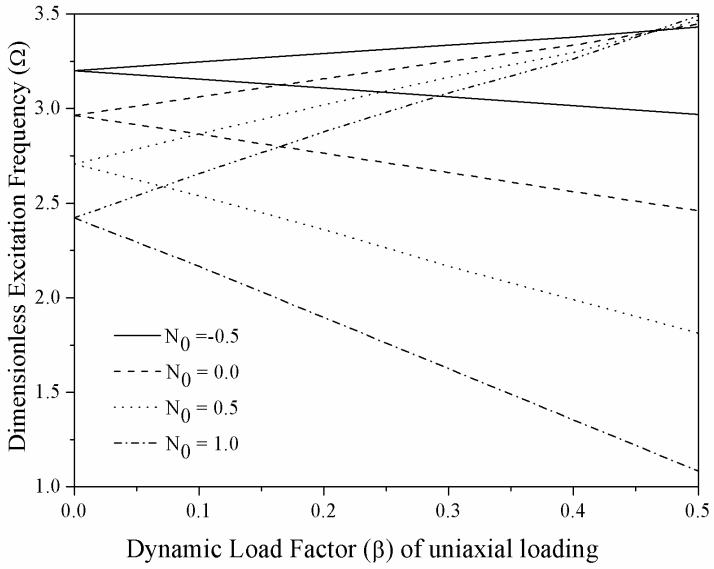

Fig. 11 Principal instability zones of SSSS three layered cross-ply [0/90/0] composite skew plates (a/b=1, a/h=100, ψ=30°) subjected to parabolic biaxial in-plane loading

static load factor (α). In the present investigation, the effect of biaxial parabolic in-plane loading of a three layered cross-ply [0/90/0] composite skew plate (a/b=1, a/h=100, ψ=30°) has also been studied. The biaxial edge loading is denoted by the load ratio $N_0 (= \frac{N_{xx}}{N_{yy}})$ which is the ratio of compressive edge load in the x-direction (N_{xx}) to compressive (positive) or tensile (negative) edge load in the y-direction ($\pm N_{yy}$). For a dynamic load factor (β) of 0.4, the width of the primary instability zones are, $0.3605 \frac{\pi^2 h}{pa^2}\sqrt{\frac{E_{22}}{\rho}}$, $0.7741 \frac{\pi^2 h}{pa^2}\sqrt{\frac{E_{22}}{\rho}}$ $1.3216 \frac{\pi^2 h}{pa^2}\sqrt{\frac{E_{22}}{\rho}}$ and $2.132 \frac{\pi^2 h}{pa^2}\sqrt{\frac{E_{22}}{\rho}}$ for $N_0 (= \frac{N_{xx}}{N_{yy}}) = -0.5$, 0, 0.5 and 1 respectively. Here, because of tensile loading in y-direction, the width of instability zone becomes narrower and this has been reflected in Fig. 11.

4. Conclusions

Parametric resonance of composite skew plates for various skew angles and support conditions based on higher order shear deformation theory (HSDT) subjected to non-uniform (parabolic) and linearly varying in-plane loading is studied. The total energy functional is derived and transformed from physical domain to computational domain using transformation equation. This functional is solved using Rayleigh-Ritz method with boundary characteristics orthonormal polynomials (BCOPs) functions. The parametric resonance regions are traced for the governing differential equation by following Bolotin's method. The principal instability region is wider and has greater practical importance than other instability regions. Higher order approximation is required for

finding accurate instability zone for higher dynamic load factor. The instability region becomes wider with increases of skew angle. The width of instability obtained for uniform in-plane loading is more than linearly varying loadings and parabolic loading. The width of instability zone decreases with decrease of span to thickness ratio and increases with the increase of aspect ratio. For pure bending in-plane loading, the skew plate becomes unstable at a higher excitation frequency compared to other linearly varying in-plane loading. The instability zones become narrower with increase of edge restraint. The width of zone of instability is the maximum for skew plates with simply support in all four edges and minimum for clamped supported in all four edges. The width of zone of instability increases with the increase of static load factor. For biaxial loading, because of tensile loading at one edge of the skew plate and compression at other edge, the width of instability zone becomes narrower.

References

Bert, C.W. and Birman, V. (1987), "Dynamic instability of shear deformable antisymmetric angle-ply plates", *Int. J. Solid. Struct*., **23**(7), 1053-1061.

Babu, S.C. and Kant, T. (1999), "Two shear deformable finite element models for buckling analysis of skew fibre-reinforced composite and sandwich panels", *Compos. Struct*., **46**(2), 115-124.

Bolotin V.V. (1964), *The Dynamic Stability of Elastic Systems*, Holden-day, San Francisco.

Chen, L.W. and Yang, J.Y. (1990), "Dynamic stability of laminated composite plates by the finite element method", *Comput. Struct*., **36**(5), 845-851.

Chen, C.S., Tsai, T.C., Chen, W.R. and Wei, C.L. (2013), "Dynamic stability analysis of laminated composite plates in thermal environments", *Steel Compos. Struct*., **15**(1), 57-79.

Dey, P. and Singha, M.K. (2006), "Dynamic stability of composite skew plate subjected to periodic in plane load", *Thin Wall. Struct*., **44**(9), 937-942.

Durvasula, S. (1970), "Buckling of clamped skew plates", *AIAA J.*, **8**(1) 178-181.

Durvasula, S. (1971), "Buckling of simply supported skew plates", *J. Eng. Mech. Div.*, **97**(3), 967-979.

Ganapathi, M., Boisse, P. and Solaut, D. (1999), "Nonlinear dynamic stability analysis of composite laminates under periodic in-plane compressive loads", *Int. J. Numer. Meth. Eng*., **46**(6), 943-956.

Kumar, Y. and Lal, R. (2011), "Buckling and vibration of orthotropic nonhomogeneous rectangular plates with bilinear thickness variation", *J. Appl. Mech*., **78**(6), 061012.

Lee, S.Y. (2010), "Finite element dynamic stability analysis of laminated composite skew plates containing cutouts based on HSDT", *Compos. Sci. Tech*., **70**(8), 1249-1257.

Liao, C.L. and Cheng, C.R. (1994), "Dynamic stability of stiffened laminated composite plates and shells subjected to in-plane pulsating forces", *J. Sound Vib.*, **174**(3), 335-351.

Liew, K.M. and Lam, K.Y. (1990), "Application of two-dimensional orthogonal plate function to flexural vibration of skew plates", *J. Sound Vib.*, **139**(2), 242-252.

Merritt, R.G. and Willems, N. (1973), "Parametric resonance of skew stiffened plates", *J. Appl. Mech.*, **40**(2), 439-444.

Moorthy, J., Reddy, J.N. and Plaut, R.H. (1990), "Parametric instability of laminated composite plates with transverse shear deformation", *Int. J. Solid. Struct*., **26**(7), 801-811.

Noh, M.H. and Lee, S.Y. (2014), "Dynamic instability of delaminated composite skew plates subjected to combined static and dynamic loads based on HSDT", *Compos. Part B*, **58**, 113-121.

Panda, S.K. and Ramachandra, L.S. (2010), "Buckling of rectangular plates with various boundary conditions loaded by non-uniform in-plane loads", *Int. J. Mech. Sci.*, **52**(6), 819-828.

Patel, S.N., Datta, P.K. and Sheikh, A.H. (2006), "Dynamic instability analysis of laminated composite stiffened shell panels subjected to in-plane harmonic edge loading", *Struct. Eng. Mech.*, **22**(4), 483-510.

Radu, A.G. and Chattopadhyay, A. (2002), "Dynamic stability of composite plates incuding delaminations

using a higher order theory and transformation matrix approach", *Int. J. Solid. Struct*., **39**(7), 1949-1965.
Prakash, T. and Ganapathi, M. (2005), "Dynamic instability of functionally graded material plates subjected to aero-thermo-mechanical loads", *Struct. Eng. Mech.*, **20**(4), 435-450.
Ramachandra, L.S. and Panda, S.K. (2012), "Dynamic instability of composite plates subjected to non-uniform in-plane loads", *J. Sound Vib*., **331**(1), 53-65.
Reddy, J.N. and Liu, C.F. (1985), "A higher-order shear deformation theory of laminated elastic shells", *Int. J. Eng. Sci.*, **23**(3), 319-330.
Reddy, J.N. (2004), *Mechanics of Laminated Composite Plates and Shells: Theory and Analysis*, 2nd Edition, CRC Pres, Boca Raton.
Reddy, J.N. (2007), *Theory and Analysis of Elastic Plates and Shells*, Taylor and Francis.
Singh, B. and Chakraverty, S. (1994), "Flexural vibration of skew plates using boundary characteristic orthogonal polynomials in two variables", *J. Sound Vib.*, **173**(2), 157-178.
Soldatos, K.P. (1991), "A refined laminated plate and shell theory with applications", *J. Sound Vib*., **144**(1), 109-129.
Srinivasan, R.S. and Chellapandi, P. (1986), "Dynamic stability of rectangular laminated composite plates", *Comput. Struct*., **24**(2), 233-238.
Timoshenko, S.P and Goodier, J.N. (1970), *Theory of elastic stability*, McGraw-Hill, New York.
Takahashi, K. and Konishi, Y. (1988), "Dynamic stability of rectangular plate subjected to distributed in-plane dynamic force", *J. Sound Vib.*, **123**(1), 115-127.
Udar, R.S. and Datta, P.K. (2007), "Dynamic combination resonance characteristics of doubly curved panels subjected to non-uniform tensile edge loading with damping", *Struct. Eng. Mech*., **25**(4), 481.
Wang, C.M., Liew, K.M. and Alwis, W.A.M. (1992), "Buckling of skew plates and corner condition for simply supported edges", *J. Eng. Mech*., **118**(4), 651-662.
Wang, H., Chen C.S. and Fung, C.P. (2013), "Hygrothermal effects on dynamic instability of a laminated late under an arbitrary pulsating load", *Struct. Eng. Mech*., **48**(1), 103-124.
Wang, S. (1997), "Buckling analysis of skew fibre-reinforced composite laminates based on first-order shear deformation plate theory", *Comput. Struct*., **37**(1), 5-19.
Wang, X., Wang, X. and Shi, X. (2007), "Accurate buckling loads of thin rectangular plates under parabolic edge compressions by the differential quadrature method", *Int. J. Mech. Sci*., **49**(4), 447-453.
Wu, G.Y. and Shih, Y.S. (2006), "Analysis of dynamic instability of arbitrarily laminated skew plates", *J. Sound Vib*., **292**(1), 315-340.

CC

Appendix A

$$
\begin{aligned}
f_1(u^o_{,\xi},u^o_{,\eta},v^o_{,\xi},v^o_{,\eta}) &= \frac{1}{a^2}(A_{11}+A_{66}\tan^2\psi)(u^o_{,\xi})^2-\frac{2}{ab}A_{66}\tan\psi\sec\psi u^o_{,\xi}u^o_{,\eta}\\
&+\frac{1}{b^2}A_{66}\sec^2\psi(u^o_{,\eta})^2-\frac{2}{a^2}(A_{11}+A_{66})\tan\psi u^o_{,\xi}v^o_{,\xi}+\frac{2}{ab}A_{12}\sec\psi u^o_{,\xi}v^o_{,\eta}\\
&+\frac{2}{ab}A_{66}\sec\psi u^o_{,\eta}v^o_{,\xi}+\frac{1}{a^2}(A_{22}\tan^2\psi+A_{66})(v^o_{,\xi})^2-\frac{2}{ab}A_{22}\tan\psi\sec\psi v^o_{,\xi}v^o_{,\eta}\\
&+\frac{1}{b^2}A_{22}\sec^2\psi(v^o_{,\eta})^2
\end{aligned}
\tag{A.1}
$$

$$
\begin{aligned}
f_2(w^o_{,\xi\xi},w^o_{,\xi\eta},w^o_{,\eta\eta},\phi^o_{1,\xi},\phi^o_{1,\eta},\phi^o_{2,\xi},\phi^o_{2,\eta}) &= \frac{1}{a^4}(D_{11}+2D_{12}\tan^2\psi+4D_{66}\tan^2\psi\\
&+D_{22}\tan^4\psi)(w^o_{,\xi\xi})^2-\frac{4}{a^3b}(D_{12}+2D_{66}+D_{22}\tan^2\psi)\tan\psi\sec\psi w^o_{,\xi\xi}w^o_{,\xi\eta}\\
&+\frac{2}{a^2b^2}(D_{12}+D_{22}\tan^2\psi)\sec^2\psi w^o_{,\xi\xi}w^o_{,\eta\eta}+\frac{4}{a^2b^2}(D_{66}+D_{22}\tan^2\psi)\sec^2\psi(w^o_{,\xi\eta})^2\\
&-\frac{4}{ab^3}D_{22}\tan\psi\sec^3\psi w^o_{,\xi\eta}w^o_{,\eta\eta}+\frac{1}{b^4}D_{22}\sec^4\psi(w^o_{,\eta\eta})^2-\frac{1}{a^3}(E_{11}+E_{12}\tan^2\psi\\
&+2E_{66}\tan^2\psi)w^o_{,\xi\xi}\phi^o_{1,\xi}+\frac{2}{a^2b}E_{66}\tan\psi\sec\psi w^o_{,\xi\xi}\phi^o_{1,\eta}+\frac{1}{a^3}(E_{12}+2E_{66}\\
&+E_{22}\tan^2\psi)\tan\psi w^o_{,\xi\xi}\phi^o_{2,\xi}-\frac{1}{a^2b}(E_{12}+E_{22}\tan^2\psi)\sec\psi w^o_{,\xi\xi}\phi^o_{2,\eta}\\
&+\frac{2}{a^2b}(E_{12}+E_{66})\tan\psi\sec\psi w^o_{,\xi\eta}\phi^o_{1,\xi}-\frac{2}{ab^2}E_{66}\sec^2\psi w^o_{,\xi\eta}\phi^o_{1,\eta}\\
&-\frac{2}{a^2b}(E_{66}+E_{22}\tan^2\psi)\sec\psi w^o_{,\xi\eta}\phi^o_{2,\xi}+\frac{2}{ab^2}E_{22}\tan\psi\sec^2\psi w^o_{,\xi\eta}\phi^o_{2,\eta}\\
&-\frac{1}{ab^2}E_{12}\sec^2\psi w^o_{,\eta\eta}\phi^o_{1,\xi}+\frac{1}{ab^2}E_{22}\tan\psi\sec^2\psi w^o_{,\eta\eta}\phi^o_{2,\xi}-\frac{1}{b^3}E_{22}\sec^3\psi w^o_{,\eta\eta}\phi^o_{2,\eta}
\end{aligned}
\tag{A.2}
$$

$$
\begin{aligned}
f_3(w^o_{,\xi\xi},w^o_{,\xi\eta},w^o_{,\eta\eta},\phi^o_{1,\xi},\phi^o_{1,\eta},\phi^o_{2,\xi},\phi^o_{2,\eta}) &= -\frac{1}{a^3}(E_{11}+E_{12}\tan^2\psi\\
&+2E_{66}\tan^2\psi)w^o_{,\xi\xi}\phi^o_{1,\xi}+\frac{2}{a^2b}E_{66}\tan\psi\sec\psi w^o_{,\xi\xi}\phi^o_{1,\eta}+\frac{1}{a^3}(E_{12}\\
&+2E_{66}+E_{22}\tan^2\psi)\tan\psi w^o_{,\xi\xi}\phi^o_{2,\xi}-\frac{1}{a^2b}(E_{12}+E_{22}\tan^2\psi)\sec\psi w^o_{,\xi\xi}\phi^o_{2,\eta}\\
&+\frac{2}{a^2b}(E_{12}+E_{66})\tan\psi\sec\psi w^o_{,\xi\eta}\phi^o_{1,\xi}-\frac{2}{ab^2}E_{66}\sec^2\psi w^o_{,\xi\eta}\phi^o_{1,\eta}\\
&-\frac{2}{a^2b}(E_{66}+E_{22}\tan^2\psi)\sec\psi w^o_{,\xi\eta}\phi^o_{2,\xi}+\frac{2}{ab^2}E_{22}\tan\psi\sec^2\psi w^o_{,\xi\eta}\phi^o_{2,\eta}\\
&-\frac{1}{ab^2}E_{12}\sec^2\psi w^o_{,\eta\eta}\phi^o_{1,\xi}+\frac{1}{ab^2}E_{22}\tan\psi\sec^2\psi w^o_{,\eta\eta}\phi^o_{2,\xi}-\frac{1}{b^3}E_{22}\sec^3\psi w^o_{,\eta\eta}\phi^o_{2,\eta}
\end{aligned}
$$

$$+\frac{1}{a^2}(F_{11}+F_{66}\tan^2\psi)(\phi^o_{1,\xi})^2-\frac{2}{ab}F_{66}\tan\psi\sec\psi\phi^o_{1,\xi}\phi^o_{1,\eta}+\frac{1}{b^2}F_{66}\sec^2\psi(\phi^o_{1,\eta})^2$$
$$-\frac{2}{a^2}(F_{11}+F_{66})\tan\psi\phi^o_{1,\xi}\phi^o_{2,\xi}+\frac{2}{ab}F_{12}\sec\psi\phi^o_{1,\xi}\phi^o_{2,\eta}+\frac{2}{ab}F_{66}\sec\psi\phi^o_{1,\eta}\phi^o_{2,\xi} \tag{A.3}$$
$$+\frac{1}{a^2}(F_{22}\tan^2\psi+A_{66})(\phi^o_{2,\xi})^2-\frac{2}{ab}F_{22}\tan\psi\sec\psi\phi^o_{2,\xi}\phi^o_{2,\eta}+\frac{1}{b^2}F_{22}\sec^2\psi(\phi^o_{2,\eta})^2$$

$$f_4(\phi^o_1,\phi^o_2)=H_{44}(\phi^o_2)^2+H_{55}(\phi^o_1)^2 \tag{A.4}$$

$$\begin{aligned}f_5(n_{xx},n_{xy},n_{yy},w^o_{,\xi},w^o_{,\eta})&=(\frac{n_{xx}}{a^2}-\frac{2n_{xy}}{ab}\tan\psi+\frac{n_{yy}}{b^2}\tan^2\psi)(w^o_{,\xi})^2\\&+(\frac{2n_{xy}}{ab}\sec\psi-\frac{2n_{yy}}{b^2}\tan\psi\sec\psi)w^o_{,\xi}w^o_{,\eta}+\frac{n_{yy}}{b^2}\sec^2\psi(w^o_{,\eta})^2\end{aligned} \tag{A.5}$$

$$f_6(u^o_{,t},v^o_{,t},w^o_{,t},\phi^o_{1,t},\phi^o_{2,t})=\rho h[(u^o_{,t})^2+(v^o_{,t})^2+(w^o_{,t})^2]+\frac{\rho h^3}{12}[(\phi^o_{1,t})^2+(\phi^o_{2,t})^2] \tag{A.6}$$